

Cu₂O photocathodes for photoelectrochemical water splitting

Author: Mar Monguilod Cuevas

Facultat de Física, Universitat de Barcelona, Diagonal 645, 08028 Barcelona, Spain.

Advisor: Cristian Fabrega Gallego and Teresa Andreu Arbella

Abstract: Photoelectrochemical water splitting is a promising technique for obtaining hydrogen through solar energy. In this work we have synthesized Cu₂O photocathodes through electrodeposition and passivated them with heat treatment and a thin electrodeposited ZnO layer. Chronoamperometries and linear sweep voltammetries have been performed to analyze their photoelectrochemical performance. The photocathodes have also been characterized by Scanning Electron Microscopy, Raman and UV-vis spectroscopy.

I. INTRODUCTION

With the increase of CO₂ emissions there has been a rising need to find alternative solutions to society's energy demands. The link between CO₂ emissions and hydrogen is the following: in order to reduce CO₂ emissions we need renewable energy sources but we also need new alternatives to store that energy, H₂ is one of those alternatives [1].

Photoelectrochemical (PEC) water splitting consists of obtaining hydrogen through the separation of water with solar energy. PEC cells are composed of two electrodes (a cathode and an anode, at least one of which is a semiconductor) submerged in a water-based electrolyte. If we are working with a p-type semiconductor, we will have a photocathode that absorbs light and generates electron and hole pairs. The electrons will then reduce the H₂O releasing H₂.

Some challenges that photoelectrochemical water splitting faces are the high cost of the materials used and their low efficiency, which complicates its scalability.

Thanks to its low cost and band gap, Cu₂O is a promising option for a water splitting photocathode. It is a p-type semiconductor with a band gap of 2-2.6 eV [2], allowing the material to have a broad absorption band of the solar spectrum. The redox potential of H₂O, as seen in Figure 1, is within the Cu₂O's bandgap. This means that the electrons accumulated at the semiconductor-electrolyte interface due to Cu₂O's p-type nature can be used in the redox reactions, which makes Cu₂O photocathodes a great option for water splitting [1]. Unfortunately it suffers from two main drawbacks:

1. Cu₂O photocathodes experience photocorrosion because the redox potentials of Cu and CuO are within the Cu₂O's bandgap. This means that the Cu₂O oxidizes and turns to CuO or reduces and turns to metallic copper because it is more stable in that form.
2. Cu₂O has a fast hole and electron recombination rate, meaning that not all the charge carriers are extracted therefore the photocurrent decreases.

To mitigate these drawbacks, two strategies can be followed: adding a minority carrier transport layer and/or

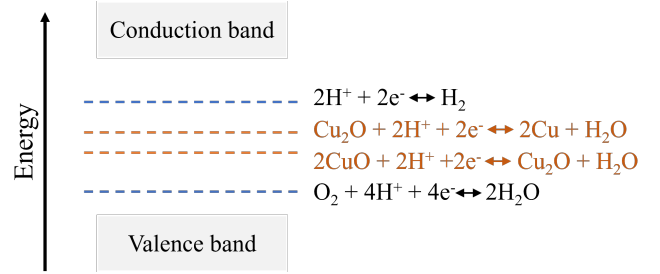


Figure 1: Positions of water's redox potentials (blue) and Cu₂O's corrosion potentials (orange) with respect to the conduction and valence band of Cu₂O [1].

adding a protective layer [3]. Since Cu₂O is a p-type semiconductor, its minority carriers are electrons therefore the minority carrier transport layer should consist of an n-type material. The protective layer must be chemically and electrochemically stable in the working electrolyte. Some materials can act as these two layers at the same time, such as ZnO, which is an n-type material stable in electrolytes with moderate pH. The energy bands of the Cu₂O/ZnO can be seen in Figure 2, we can also appreciate how the ZnO acts as an electron transport layer: when the two layers are in contact the electrons will move towards the electrolyte and the holes towards the FTO.

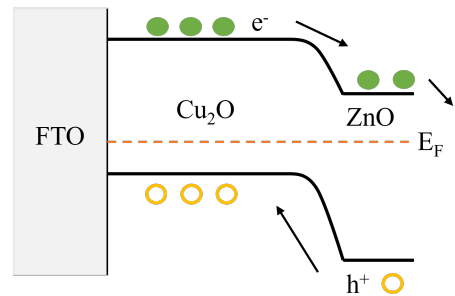


Figure 2: Energy band diagram for the Cu₂O/ZnO photocathode.

II. EXPERIMENTAL SECTION

A. Materials

1. Electrodeposition of Cu₂O

The electrodeposition was performed using a multichannel Biologic SP-150 potentiostat with a two-electrode configuration. The FTO glass substrate was used as the working electrode and a mesh of platinum was used as the counter electrode. The plating solution consisted of 0.2M CuSO₄ · 5 H₂O, 3M C₃H₆O₃, and 0.5M K₂HPO₄ · 3 H₂O and its pH was adjusted to 12 with 3M KOH. The electrodeposition was performed at a constant current of -1 mA/cm^2 at 60°C. The sample's thickness was controlled with the electrodeposition time (15, 30, 45, 60, and 75 min).

2. Annealing of the Cu₂O photocathodes

After Cu₂O electrodeposition, some photocathodes were annealed for 1 hour at 350 °C in N₂ atmosphere, at a rate of 10 °C/min.

3. Electrodeposition of ZnO on Cu₂O photocathodes

The electrodeposition was performed on top of the Cu₂O photocathodes using a multichannel Biologic SP-150 potentiostat with a two-electrode configuration. The counter electrode was a platinum mesh. For the plating solution 50mM Zn(NO₃)₂ · 6 H₂O and 100mM of p-benzoquinone were dissolved in 20 mL of dimethyl sulfoxide. The electrodeposition was performed at a constant current of -0.11 mA/cm^2 during 7 min 34 s.

B. Material characterization

Optical characterization was performed with a UV-Vis-IR Perkin Elmer Lambda 950 spectrophotometer with a 150 mm integrating sphere. The surface morphology and the cross section of the samples were observed using a field emission scanning electron microscope (FESEM, JEOL J-7100). Raman spectroscopy were recorded using a Jobin-Yvon LabRaman HR 800 dispersive spectrometer with a green laser and an ultraviolet laser. Both FESEM and Raman measurements were carried out in the CCTiUB facilities.

C. Photoelectrochemical characterization

Photoelectrochemical (PEC) measurements were conducted in a three-electrode system using a Biologic VSP-300 potentiostat. An optical glass cell with a platinum

mesh as the counter electrode and Ag/AgCl (3.5M) ($E^0 = 0.205 \text{ V vs RHE}$) as the reference electrode was used for this purpose. Part of the samples were covered in nail polish so there was no contact between the electrolyte and the FTO substrate. The electrolyte consisted of 0.5M Na₂SO₄ and for some measurements H₂O₂ was used as an electron scavenger.

Chronoamperometric measurements were performed at a constant potential of $-0.3 \text{ V vs Ag/AgCl}$ and light pulses of 20 s supplied by a Newport LED solar simulator LSH-7320 with a 400-1100 nm range coupled with a SHB1T Thorlabs diaphragm shutter. Linear sweep voltammeteries from 0.3 V to $-0.6 \text{ V vs Ag/AgCl}$ were recorded under light pulses of 1 s at a scan rate of 20 mV/s.

III. RESULTS AND DISCUSSION

A. Structural characterization

SEM images were taken in order to study the structure of the samples. Figure 3a-c shows the morphology of the different films obtained through the electrodeposition methods. We can observe that all the samples are homogeneous and the layer of bare Cu₂O (Figure 3 a) has a cubic morphology. After exposing the bare Cu₂O samples to heat treatment (Figure 3 b) they become more granular while maintaining the cubic morphology. Figure 3 c shows a sample that has been electrodeposited with ZnO after annealing the bare Cu₂O photocathode,

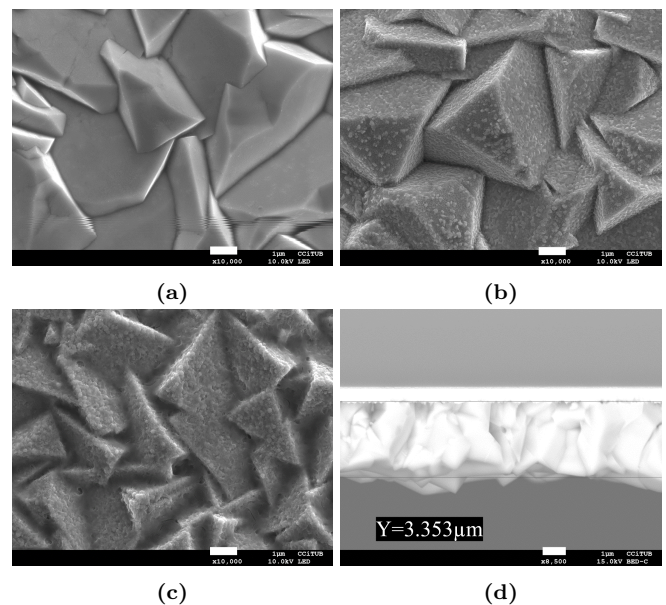


Figure 3: FESEM images of (a) electrodeposited Cu₂O on top of FTO, (b) electrodeposited Cu₂O on top of FTO after annealing, (c) electrodeposited ZnO on top of annealed Cu₂O and (d) cross section of the bare Cu₂O photocathode. Scale bar represents 1 μm.

we can appreciate the presence of ZnO with the thin veil that forms on top of the annealed Cu₂O.

Before passivating and adding the ZnO layer we created a series of samples with different electrodeposition times, ranging from 15 min to 75 min. With cross section images we concluded that the thickness of the samples increased with the electrodeposition time in a non linear way. We chose to work with the 45 min samples because they had a higher photocurrent than the rest. Figure 3 d shows the cross section of a bare Cu₂O sample electrodeposited during 45 min, the white section at the top is the FTO substrate and the bottom section is the Cu₂O. The thickness of the Cu₂O is about 3.35 μm .

B. Chemical characterization

Figure 4 shows the Raman spectra of the different samples, which we used to determine their structure. Figure 4 (top) displays the spectra of Cu₂O with and without annealing with the Raman shift peaks identified. We concluded that the peaks corresponding to Cu₂O are at 218, 412, 516 and 628 cm^{-1} , all of them present in the bare Cu₂O photocathode [4]. As for the annealed samples, even though they were annealed in N₂ atmosphere, we can see an extra peak at 297 cm^{-1} corresponding to CuO, which means that some oxidation occurred. This might have happened due to some residual oxygen being present during the heat treatment.

In order to see the presence of ZnO, we obtained additional Raman spectra with an ultraviolet laser instead of the green laser that was used in Figure 4(top). The results are displayed in Figure 4(bottom). The peaks at 575 and 1146 cm^{-1} correspond to ZnO and can be both seen in the ZnO electrodeposited samples [5]. Furthermore, this spectra confirmed that annealing oxidates the samples thus a peak appears at 298 cm^{-1} only in the samples subjected to heat treatment.

C. Optical characterization

In order to estimate the energy gap of the Cu₂O photocathodes we measured the total transmittance and reflectance obtained with the UV-vis measurements. We followed two methods to determine the E_{gap} : obtaining the value directly from the transmittance spectra and using the Kubelka-Munk approximation of the Tauc plot for the reflectance and the absorbance spectra.

For the first method we made a linear regression with the values where the transmittance decreased substantially, which is where the material's gap lies. The E_{gap} is the x-intercept.

For the second method we used the reflectance spectra and also the absorbance spectra, since $A = 1 - R - T$. The Kubelka-Munk approximation of the Tauc plot can

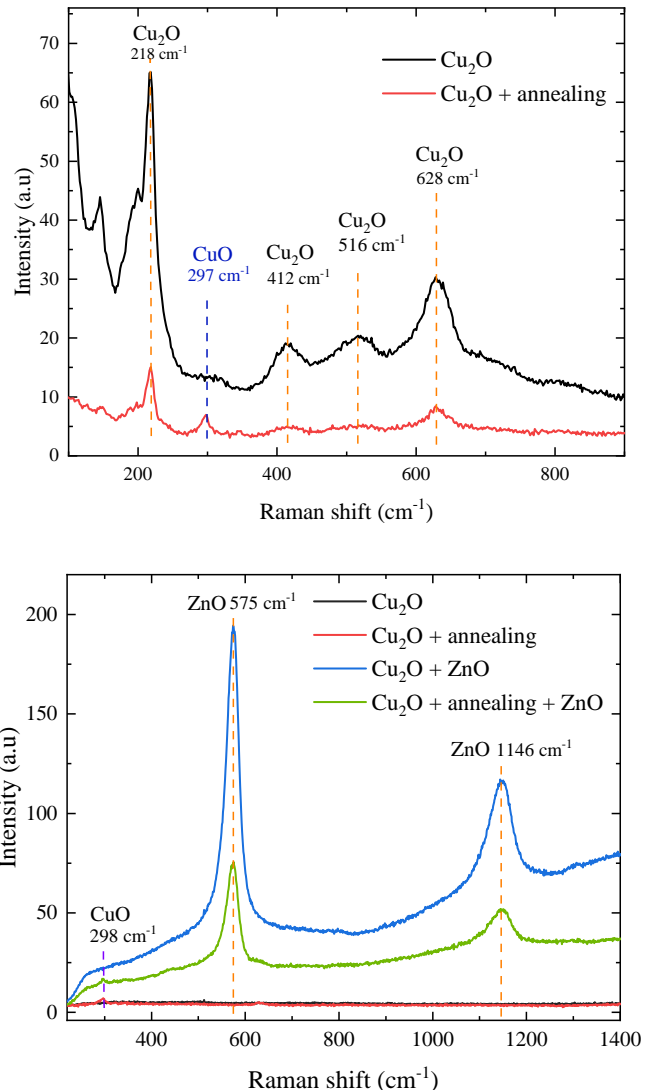


Figure 4: Raman spectra of (top) Cu₂O photocathode (black plot) and the annealed Cu₂O photocathode (red plot) and (bottom) Cu₂O photocathode (black plot), the annealed Cu₂O photocathode (red plot), the Cu₂O/ZnO photocathode (blue plot) and the Cu₂O(annealed)/ZnO photocathode (green plot). The top spectra was measured with a green laser ($\lambda = 532 \text{ nm}$) and the bottom spectra was measured with an ultraviolet laser.

be expressed as [6]:

$$(F(R)h\nu)^{1/\gamma} = B(h\nu - E_{gap}) \quad \text{where} \quad F(R) = \frac{(1-R)^2}{2R}$$

γ is 0.5 for a direct bandgap and 2 for an indirect band gap. This approximation assumes that the sample is infinitely thick, therefore the transmittance is zero.

Figure 5 shows the values of E_{gap} obtained with the different techniques. From the literature we know that the Cu₂O energy gap ranges between 2 eV and 2.6 eV, although there are some discrepancies. The transmittance

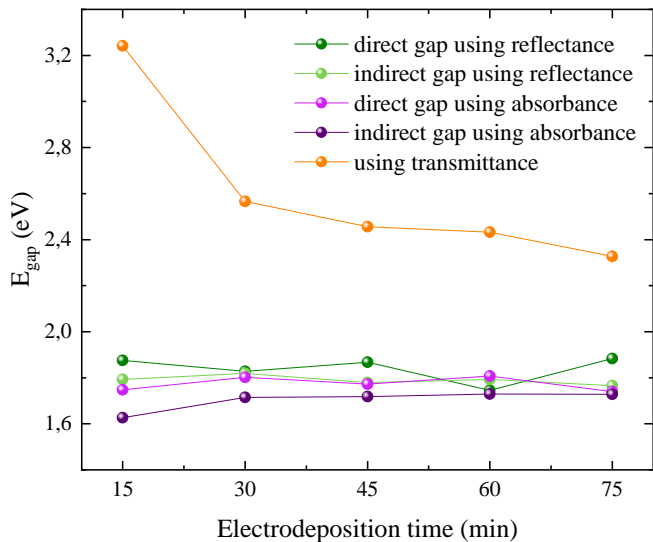


Figure 5: Values of the energy gap of the bare Cu₂O samples versus the electrodeposition time. The E_{gap} values were obtained through different approaches: through the transmittance spectra (orange plot), through the Kubelka-Munk approximation of the Tauc plot with the reflectance spectra (dark green assuming a direct band gap and light green assuming an indirect band gap) and through the Kubelka-Munk approximation of the Tauc plot with the absorbance spectra (light purple assuming a direct band gap and dark purple assuming an indirect band gap).

E_{gap} tends to 2.4 eV and the E_{gap} using the Kubelka-Munk approximation of the Tauc plot ranges between 1.6 eV and 1.9 eV. The underestimation of the gap value using the Tauc plot is probably due to our samples not being infinitely thick, therefore not being a very appropriate fit for the Kubelka-Munk approximation. On the other hand, the values obtained with the transmittance spectra, fall within the expected range.

D. Photoelectrochemical measurements

We studied the photoelectrochemical activity of the samples with chronoamperometry and linear sweep voltammetry techniques.

We conducted a chronoamperometry at -0.3 V vs Ag/AgCl with light pulses of 20 s. Figure 6 shows the results of the four different samples without and with H₂O₂, which works as an electron scavenger. We have subtracted the dark current of each sample for a better comparison but it is worth mentioning that the Cu₂O and Cu₂O/ZnO samples had the highest dark current.

The form of the pulses in Figure 6(top) give us an idea of the charge accumulation [7]. The bare Cu₂O photocathode and the Cu₂O/ZnO photocathode have very long and defined peaks at the start and end of the pulse, meaning that the charge accumulates at the surface and is not able to be collected by the electrolyte. In con-

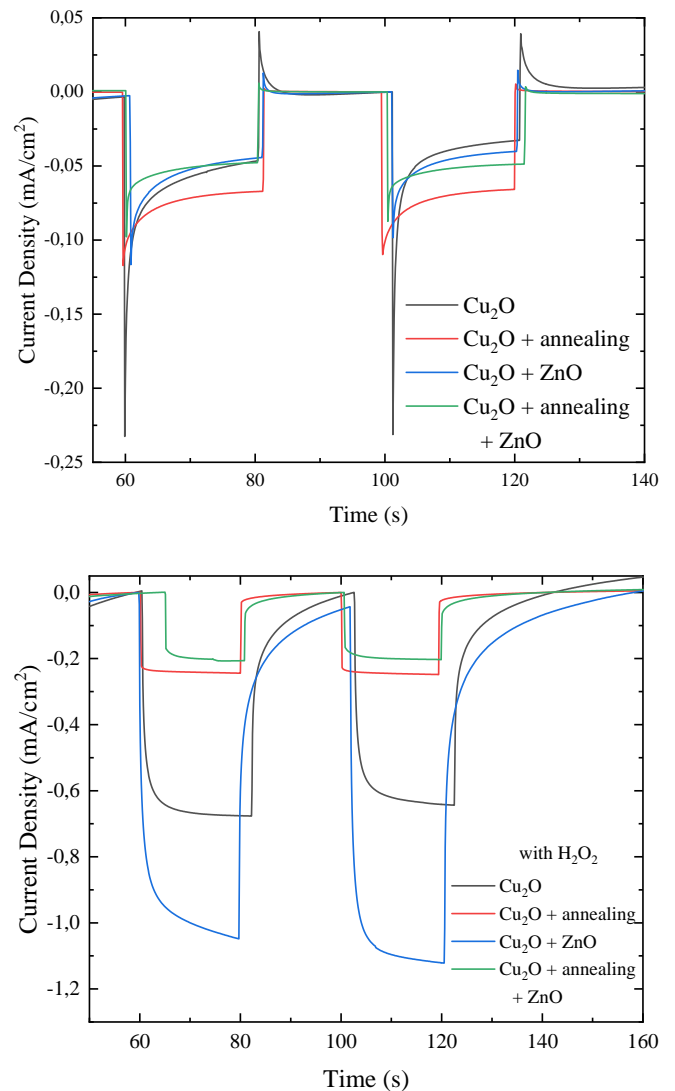


Figure 6: Chronoamperometries of the four different photocathodes performed in (top) 0.5M Na₂SO₄ and (bottom) 0.5M Na₂SO₄ and H₂O₂. The first pulse of light has been removed and the dark current of each sample has been subtracted.

trast, both of the annealed samples have a lower peak indicating that the accumulated charge is lower.

Figure 6(bottom) shows the results of the chronoamperometry when it is performed in a medium with H₂O₂. Since the peroxide is an electron scavenger this measurements allow us to see how the samples would perform with a good catalyst. We can see that the pulses are more stable than in Figure 6(top) and have a higher current. The Cu₂O/ZnO photocathode has the highest photocurrent followed by the bare Cu₂O sample, yet their stability is not as good as the annealed samples. On the other hand, the annealed Cu₂O and the annealed Cu₂O with ZnO have a lower photocurrent but a better stability. The difference between the annealed samples and the not-annealed ones might be due to the oxidation that

occurs with annealing. It is possible that the layer that appears of CuO acts as a blocking layer impeding charge transfer, therefore having a lower yet more stable photocurrent.

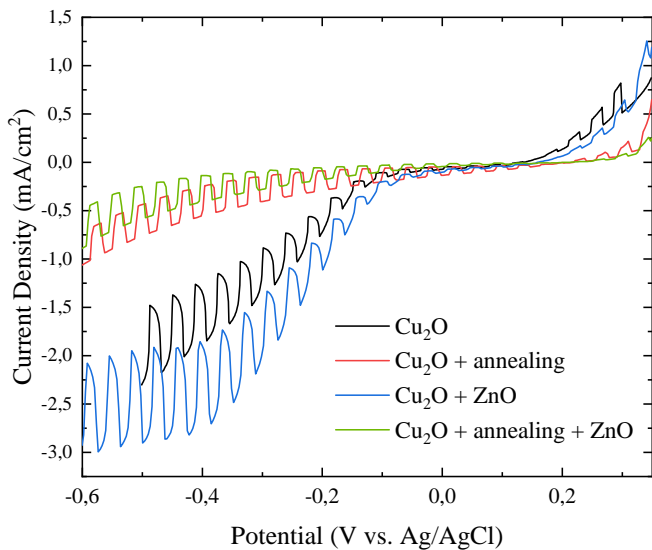


Figure 7: Linear sweep voltammeteries obtained with the four photocathodes in 0.5M Na₂SO₄ with H₂O₂ as an electron scavenger.

We performed a linear sweep voltammetry from 0.3V to -0.6 V vs Ag/AgCl with the exception of the bare Cu₂O photocathode whose voltammetry we performed from 0.3 V to -0.5 V vs Ag/AgCl in order to avoid damaging the sample with corrosion. The results are shown in Figure 7 and they are coherent with the observations of the chronoamperometry: the bare Cu₂O and the Cu₂O/ZnO photocathodes have the highest photocurrent but also the highest dark current and lowest stability, meanwhile the annealed photocathodes show a lower photocurrent as well as a lower dark current and higher stability.

IV. CONCLUSIONS

We successfully obtained four different samples by electrodepositing Cu₂O on FTO, annealing some of the Cu₂O photocathodes and electrodepositing ZnO on the annealed and not annealed Cu₂O photocathodes. We were able to control the thickness of the samples with the electrodeposition time and we ended up using the 45 min samples, which correspond to a thickness of 3.353 μ m.

With the material characterization we found that the samples have a cubic structure and are homogeneous, we confirmed that we had Cu₂O and ZnO after electrodeposition and that annealing oxidated our samples so a thin layer of CuO appeared on top of the Cu₂O layer. Finally, using UV-vis spectroscopy, we estimated that the energy gap of Cu₂O photocathodes was 2.4 eV, approximately.

We also performed photoelectrochemical measurements and found that the Cu₂O/ZnO photocathode has the highest photocurrent but quite a high dark current and low stability. We can conclude that ZnO works as an electron transport layer and a protective layer but more research has to be done to lower the dark current and gain more stability in order to obtain an efficient photocathode for water splitting.

Acknowledgments

I would like to thank my advisors Dr. Cristian Fabrega and Dr. Teresa Andreu for their guidance, knowledge and dedication to this project. I would also like to thank Dr. Joan Bertomeu for his assistance with the UV-vis measurements, and Martí Molera and María González for their support and assistance in the laboratory. Finally, a special thanks to my family and friends.

-
- [1] Jinshui Cheng, Linxiao Wu, Jingshan Luo. Cuprous oxide photocathodes for solar water splitting. **2022** *Chem. Phys. Rev.* 3, 031306
 - [2] Pramod Patil Kunturu and Jurriaan Huskens. Efficient Solar Water Splitting Photocathodes Comprising a Copper Oxide Heterostructure Protected by a Thin Carbon Layer. **2019** *ACS Appl. Energy Mater.* 2019, 2, 7850–7860
 - [3] Dae Han Wi, Margaret A. Lumley, Zhaoyi Xi, Mingzhao Liu, and Kyoung-Shin Choi. Investigation of electron extraction and protection layers on Cu₂O photocathodes. **2023** *Chem. Mater.* 2023, 35, 4385–4392
 - [4] H. Solache-Carranco, G. Juárez-Díaz, M. Galván-Arellano, J. Martínez-Juárez, G. Romero-Paredes and R. Peña-Sierra. Raman Scattering and Photoluminescence Studies on Cu₂O. **2008** *Revista Mexicana de Física* 55 (5) 393–398
 - [5] Kandabara Tapily, Diefeng Gu, Helmut Baumgart, Maria Rigo and Jaetae Seo. Raman spectroscopy of ZnO thin films by atomic layer deposition. **2010** *ECS Trans.* 2010, Volume 33, Issue 2, Pages 117-123
 - [6] Patrycja Makula, Michał Pacia, and Wojciech Macyk. How To Correctly Determine the Band Gap Energy of Modified Semiconductor Photocatalysts Based on UV-Vis Spectra. **2018** *J. Phys. Chem. Lett.* 2018, 9, 23, 6814–6817
 - [7] Sebastian Murcia-López, Cristian Fabrega, Damian Monllor-Satoca, María D. Hernandez-Alonso, German Penelas-Pérez, Alex Morata, Juan R. Morante, and Teresa Andreu. Tailoring Multilayered BiVO₄ Photoanodes by Pulsed Laser Deposition for Water Splitting. **2016** *ACS Appl. Mater. Interfaces* 2016, 8, 4076-4085